Computer Methods in Biomechanics and Biomedical Engineering, 2013
Vol. 16, No. 10, 1096–1105, http://dx.doi.org/10.1080/10255842.2013.773979

Taylor & Francis
Taylor & Francis Group

Mechanisms of cell migration in the adult brain: modelling subventricular neurogenesis

A. Van Schepdael[a,b], J.M.A. Ashbourn[c], R. Beard[d], J.J. Miller[e] and L. Geris[a,f]*

[a]*Biomechanics Research Unit, Université de Liège, Liège, Belgium;* [b]*Biomechanics Section, KU Leuven, Leuven, Belgium;* [c]*Department of Engineering Science, University of Oxford, Oxford, UK;* [d]*Exeter College, University of Oxford, Oxford, UK;* [e]*St Hugh's College, University of Oxford, Oxford, UK;* [f]*Prometheus, Division of Skeletal Tissue Engineering, KU Leuven, Leuven, Belgium*

(*Received 17 October 2012; final version received 4 February 2013*)

Neurogenesis has been the subject of active research in recent years. Although the majority of neurons form during the embryonic period, neurogenesis continues in restricted regions of the mammalian brain well into adulthood. In rodent brains, neuronal migration is present in the rostral migratory stream (RMS), connecting the subventricular zone to the olfactory bulb (OB). The migration in the RMS is characterised by a lack of dispersion of neuroblasts into the surrounding tissues and a highly directed motion towards the OB. This study uses a simple mathematical model to investigate several theories of migration of neuroblasts through the RMS proposed in the literature, including chemo-attraction, chemorepulsion, general inhibition and the presence of a migration-inducing protein. Apart from the general inhibition model, all the models were able to provide results in good qualitative correspondence with the experimental observations.

Keywords: neurogenesis; mathematical model; cell migration

1. Introduction

Neurogenesis has been the subject of active research in recent years. Although the majority of neurons form during the embryonic period, neurogenesis continues in restricted regions of the mammalian brain well into adulthood (Lois and Alvarez-Buylla 1993; Luskin 1993; Taupin and Gage 2002; Ghashghaei et al. 2007). In rodent brains, neuronal migration is present in the cerebellum, the hippocampus and the rostral migratory stream (RMS). It is in this last region, connecting the subventricular zone (SVZ) to the olfactory bulb (OB), that the most extensive neuronal migration occurs during adulthood (Ghashghaei et al. 2007).

Type-B astrocytes, present in the SVZ, differentiate into type-A neuroblast precursors (Lledo et al. 2006) through a type-C cell intermediate. Type-A neuroblasts then migrate through the RMS towards the OB and after arrival in the OB, the neuroblasts migrate radially outward and differentiate into fully mature neurons. Although migration in embryonic neurogenesis is guided by radial glial cells or axon fibres, in adult neurogenesis it is observed that the type-A cells proceed in a class of movement known as 'chain migration' (Lois et al. 1996), which is neither gliophilic nor axonophilic and in which the migrating cells form and aggregate such that each cell can use its neighbouring cells as a migratory substrate.

The migration in the RMS is characterised by a lack of dispersion of neuroblasts into the surrounding tissues and a highly directed motion towards the OB. The reasons for this directed motion are currently unknown, but it has been suggested in several studies (Bloch-Gallego et al. 1999; Yee et al. 1999; Alcantara et al. 2000) that cell migration is directed chemotactically along gradients of various chemical factors distributed differentially throughout the migratory path between the SVZ and the OB. Murase and Horwitz (2002) reported on a study that tested the hypothesis that the molecule netrin-1, which is produced by olfactory mitral cells, may function to provide a chemogradient through the forebrain that attracts migrating cells to the OB. The attractive effect of netrin-1 on SVZ neuronal migration has also been shown in vitro (Alcantara et al. 2000; Mason et al. 2001). However, cells migrate successfully even in the absence of the OB (Jankovski et al. 1998), although the magnitude of migration is greatly reduced. This implies that long-distance attractive signals from the OB are not necessary for oriented migration, suggesting that a different, currently unknown mechanism is responsible for neuronal migration.

It has also been proposed that instead of chemo-attraction, a form of chemorepulsion mediated by SLIT proteins might be involved in the migration of astrocytes in the RMS (Hu 1999; Wu et al. 1999; Ghashghaei et al. 2007). SLIT proteins are secreted by cells surrounding the SVZ, and the SLIT-receptors ROBO 1, 2 and 3 are expressed in the SVZ (Wu et al. 1999; Marillat et al. 2002; Nguyen-Ba-Charvet et al. 2004; Ghashghaei et al. 2007). Thus, when exposed to SLIT, cells might turn away from the SVZ and initiate migration through the RMS.

This proposal was later investigated by Mason et al. (2001), who inferred from their experimental findings that SLIT may instead serve as general migratory inhibitors, perhaps preventing SVZ neuroblasts from migrating into

*Corresponding author. Email: liesbet.geris@ulg.ac.be

certain regions of the brain, rather than serving as chemorepulsive factors. Furthermore, they showed that glial cells in the RMS secrete a protein (yet to be identified) with migration-inducing activity, which induces neuronal migration, and postulated that it is the combined effect of these proteins that leads to repulsion.

Starting from the model for adult neurogenesis developed by Ashbourn et al. (2012), we investigate the different theories of migration mentioned above. Using a mathematical model, Ashbourn et al. simulate the differentiation of neuronal precursors and the migration through the RMS – one of the hypotheses constituting their model is that migration is mainly driven by chemotaxis. In this study, we model several other migration hypotheses and study their different outcomes in terms of the resulting average cell concentration in the OB.

2. Materials and methods

2.1 *Reference model: diffusion*

As mentioned above, this study starts from the model of Ashbourn et al. (2012), in which they developed a 2D model simulating the SVZ, the OB and the RMS. Although the migration through the RMS is a complex 3D process, all experimental data available in the literature have been obtained using 2D axial slices. Ashbourn et al. therefore considered that modelling the process in two dimensions was an acceptable simplification. The computational domain takes the form of two interconnected boxes with the larger corresponding to the OB and the smaller to the SVZ, as illustrated in Figure 1. The SVZ is populated by type-B cells (n_B), which differentiate into type-A neuroblasts (n_A) through the type-C cell intermediate (n_C). Although type-B and type-C cells are assumed to be immobile, type-A cells are modelled to migrate through diffusion and through directed motion towards the OB. Ashbourn et al. (2012) specified the directed motion guiding the neuroblasts to the OB and hypothesised that it was caused by a single chemo-attractant factor (f_A) present in the OB. Once outside the SVZ, the proliferation rate of type-A cells slows down (Smith 1998) and upon arrival in the centre of the OB, type-A cells either differentiate into mature neurons (n_n) or die (Biebl et al. 2000). For computational ease, the centre of the OB is defined as a square with side b. The mature neurons finally migrate radially outwards towards the edges of the OB, and this migration is modelled as chemotaxis against a constant environmental factor g. A logistic growth term was used to model the proliferation of all cell types, and all reaction terms, differentiation and decay terms were modelled with simple linear reaction kinetics (see Equations (1)–(8)).

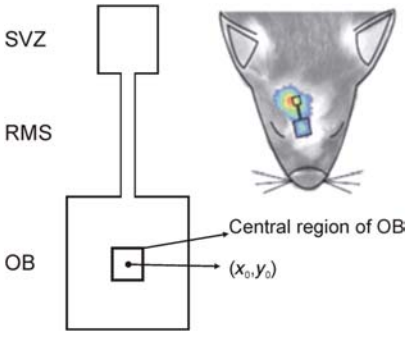

Figure 1. Domain of the model. Illustration of the computational domain and its approximate physiological location (inset bioluminescent mouse image taken from Reumers et al. (2008)).

In this study, we adopted the model of Ashbourn et al. (2012) including the parameter values and initial conditions, but we removed the chemo-attractant factor f_A. The model is then governed by Equations (1)–(8), and the initial state of cell distribution within the system comprised only a uniform supply of type-B cells throughout the SVZ. This set of equations is used as a reference model by which all hypotheses of this study are tested. The boundary conditions on all boundaries of the domain were set to zero-flux, indicating that there is no flux of cells or chemical factors between the surrounding tissue and the domain. Ashbourn et al. have extensively investigated the parameter space by means of a sensitivity analysis and a more thorough sloppy parameter analysis showing the non-uniqueness of the set of parameters providing physiological results with the proposed equations. Keeping that in mind, we used the reference parameter set of Ashbourn et al. (Table 1), in which all values are given in non-dimensionalised form. Furthermore, we did not search for exact experimentally tested parameter values for the additional Equations (9)–(19) proposed in this study, but rather inferred their values from the earlier model and verified whether the yielded solutions were physiological. Additional details on the different terms of the equations and on the parameter values can be found in Ashbourn et al. (2012).

$$\frac{\partial n_B}{\partial t} = \overbrace{\beta_B n_B(1-n_B)}^{\text{Proliferation}} - \overbrace{\alpha_C n_B}^{\text{Differentiate}} - \overbrace{\gamma_B n_B}^{\text{Apoptosis}} \tag{1}$$

$$\frac{\partial n_C}{\partial t} = \overbrace{\beta_C n_C(1-n_C)}^{\text{Proliferation}} - \overbrace{\alpha_A n_C + \alpha_C n_B}^{\text{Differentiate}} - \overbrace{\gamma_C n_C}^{\text{Apoptosis}} \tag{2}$$

$$\frac{\partial n_A}{\partial t} = \overbrace{\delta_A \nabla^2 n_A}^{\text{Diffusion}} + \overbrace{\beta_A(\mathbf{r}) n_A(1-n_A)}^{\text{Proliferaton}} + \overbrace{\alpha_A n_C - \zeta(\mathbf{r}) n_A}^{\text{Differentiate}} - \overbrace{(\gamma_A + \varepsilon(\mathbf{r})) n_A}^{\text{Apoptosis}} \tag{3}$$

Table 1. Parameter values derived from the model of Ashbourn et al. (2012).

Parameter	Parameter value
β_B	7.567
α_C	2.182
γ_B	0.701
β_C	9.411
α_A	1.700
γ_C	0.744
δ_A	0.037
δ_N	0.053
γ_A	0.737
η_N	9.136
γ_N	0.079
a_4	1.000
a_2	0.500
d	1.921
b	0.500
μ	0.213
β_{Ai}	1.735
β_{Ao}	0.785
η_A	0.134
a_1	1.000
a_3	1.000
λ	0.422
κ_D	9.284
κ_A	6.045
κ_B	1.276
κ_C	2.292
δ_{f_A}	1.955

$$\frac{\partial n_N}{\partial t} = \overbrace{\delta_N \nabla^2 n_N}^{\text{Diffusion}} - \overbrace{\nabla\cdot(\eta_N n_N \nabla g)}^{\text{Radial migration}} + \overbrace{\zeta(\mathbf{r}) n_A}^{\text{Differentiate}} - \overbrace{\gamma_N n_N}^{\text{Apoptosis}} \tag{4}$$

$$g := a_4\left(1 - \exp\left[-\left(\frac{(x-x_0)^2 + (y-y_0)^2}{a_2}\right)\right]\right) \tag{5}$$

$$\varepsilon(\mathbf{r}) := \begin{cases} d & \text{for } |x - x_0| \le b, \text{and } |y - y_0| \le b \\ 0 & \text{otherwise} \end{cases} \tag{6}$$

$$\zeta(\mathbf{r}) \propto \varepsilon(\mathbf{r}) = \mu\varepsilon(\mathbf{r}); \quad \varsigma < \varepsilon. \tag{7}$$

$$\beta_A(\mathbf{r}) := \begin{cases} \beta_{Ai} & \text{within the SVZ} \\ \beta_{Ao} & \text{otherwise.} \end{cases} \tag{8}$$

The variables in this model represent concentrations, either cells or chemical factors. It is therefore vital that the solutions to such a system are non-negative and respect conservation of mass. The finite volumes technique was used for its inherent mass conservation properties. The method of lines was applied to separate the spatial and temporal discretisation (Gerisch and Chaplain 2006) of differentials over the computational grid of 15,600 spatial points across the domain. The spatial discretisation of the diffusion and reaction terms was carried out using, respectively, the standard second order central difference approximation and pointwise evaluation. For the discretisation of the taxis terms, upwinding techniques with nonlinear limiter functions (van Leer limiter) were applied to guarantee accurate, non-negative solutions (Gerisch and Chaplain 2006; Geris et al. 2008). For the time integration of the resulting system of ordinary differential equations, the ROWMAP time integrator (Weiner et al. 1997) was used.

2.2 Chemo-attraction

The first hypothesis to be tested postulates that the directed motion towards the OB is guided by a chemo-attractant factor f_A as modelled by Ashbourn et al. (2012). This factor was assumed to be produced inside the OB at a rate

$$a_3 \exp\left\{-\left[\frac{(x-x_0)^2 - (y-y_0)^2}{a_1}\right]\right\}$$

and secreted by type-A, -B and -C cells, and the factor is assumed to be diffusible and undergoes a natural decay λf_A. Type-A cells are attracted towards a high concentration of chemo-attractant factor, which is taken up by those cells at a rate $\kappa_D f_A n_A$.

Equation (3) is thus replaced by Equation (9), adding a term representing the chemo-attraction, and Equation (10) governing the concentration of attractant factor f_A is added to the system of equations. The attractant factor f_A is assumed to have an initial 2D Gaussian distribution in the centre of the OB, with a maximum concentration of $f_A = 10$.

$$\frac{\partial n_A}{\partial t} = \delta_A \nabla^2 n_A - \overbrace{\nabla\cdot(\eta_A n_A \nabla f_A)}^{\text{Chemo-attraction}} + \beta_A(\mathbf{r}) n_A(1 - n_A) + \alpha_A n_C - \zeta(\mathbf{r}) n_A - (\gamma_A + \varepsilon(\mathbf{r})) n_A \tag{9}$$

$$\frac{\partial f_A}{\partial t} = \overbrace{\delta_{f_A} \nabla^2 f_A}^{\text{Diffusion}} + \overbrace{\kappa_A n_A + \kappa_B n_B + \kappa_C n_C}^{\text{Production}} - \overbrace{\kappa_D f_A n_A}^{\text{Uptake by cells}} - \overbrace{\lambda f_A}^{\text{Decay}} + \overbrace{a_3 \exp\left[-\left(\frac{(x-x_0)^2 + (y-y_0)^2}{a_1}\right)\right]}^{\text{OB attraction}} \tag{10}$$

2.3 Chemorepulsion

This model was derived to investigate the plausibility of the claim that the protein known as SLIT may play an important role in the directed migration of neuroblasts by

functioning as a chemorepellent factor (Hu 1999; Wu et al. 1999; Ghashghaei et al. 2007).

In the equations, the chemoattractant factor f_A was replaced by a chemorepellent factor f_R that required a change of sign in the type-A cell taxis term in Equation (9), indicating that these cells are predisposed to travel down the concentration gradient of the new chemical element. As SLIT is secreted by cells surrounding the SVZ, the boundary conditions on the edges of the SVZ were changed to Dirichlet boundary conditions, imposing a constant concentration of $f_R = 10$ at those boundaries. Furthermore, SLIT is subject to diffusion and has a natural decay rate of λf_R, assumed to be equal to the decay rate of the attractant factor f_A defined by Ashbourn et al. (2012). The diffusion constant δ_{f_R} of SLIT was estimated in such a way that a SLIT gradient inside the SVZ was present. Equations (9) and (10) are replaced by the following equations:

$$\frac{\partial n_A}{\partial t} = \delta_A \nabla^2 n_A + \overbrace{\nabla\cdot(\eta_A n_A \nabla f_R)}^{\text{Chemo-repulsion}} + \beta_A(\mathbf{r}) n_A(1 - n_A) + \alpha_A n_C - \zeta(\mathbf{r}) n_A - (\gamma_A + \varepsilon(\mathbf{r})) n_A \tag{11}$$

$$\frac{\partial f_R}{\partial t} = \overbrace{\delta_{f_R} \nabla^2 f_R}^{\text{Diffusion}} - \overbrace{\lambda f_R}^{\text{Decay}}. \tag{12}$$

2.4 General inhibition

This model was designed to investigate the legitimacy of the postulate that SLIT functions as a general migratory inhibitor rather than as a repellent factor, which does not affect the overall level of migration achieved, but rather it simply prevents migration towards its regions of expression (Mason et al. 2001).

In the chemorepulsive model, the SLIT protein was renamed as f_I, and the chemorepulsive effect of SLIT on type-A cells was no longer modelled. The diffusion constant δ_{n_A} was designed to be inversely proportional to the local concentration of SLIT proteins. The general inhibitory model is thus created by replacing Equations (11) and (12) by Equations (13) and (14), respectively, while maintaining the Dirichlet boundary conditions for the concentration of SLIT at the edges of the SVZ.

$$\frac{\partial n_A}{\partial t} = \overbrace{\nabla\left(\frac{\delta_A}{1 + f_I}\nabla n_A\right)}^{\text{Variable Diffusion}} + \beta_A(\mathbf{r}) n_A(1 - n_A) + \alpha_A n_C - \zeta(\mathbf{r}) n_A - (\gamma_A + \varepsilon(\mathbf{r})) n_A \tag{13}$$

$$\frac{\partial f_I}{\partial t} = \overbrace{\delta_{f_I} \nabla^2 f_I}^{\text{Diffusion}} - \overbrace{\lambda f_I}^{\text{Decay}} \tag{14}$$

2.5 Migration-inducing protein

This model was set up to investigate the effect of a protein called melanoma inhibitory activity (MIA), which induces and enhances neuronal migration (Mason et al. 2001; Ghashghaei et al. 2007), and which was modelled by making the diffusion constant δ_{n_A} of the neuroblast proportional to the local concentration of MIA. MIA is produced by glial cells inside the RMS (Mason et al. 2001; Ghashghaei et al. 2007), which is modelled as a constant production term. As a soluble protein, MIA is further able to diffuse through the extracellular matrix and has a natural decay rate of λf_M. As before, parameters δ_{f_M} and λ were assumed to be equal to the equivalent parameters from the chemo-attractive model. Parameter a_4 was chosen to achieve a MIA concentration $f_M \approx 10$ in the RMS.

$$\frac{\partial n_A}{\partial t} = \overbrace{\nabla(\delta_A(1 + f_M)\nabla n_A)}^{\text{Variable Diffusion}} + \beta_A(\mathbf{r}) n_A(1 - n_A) + \alpha_A n_C - \zeta(\mathbf{r}) n_A - (\gamma_A + \varepsilon(\mathbf{r})) n_A \tag{15}$$

$$\frac{\partial f_M}{\partial t} = \overbrace{\delta_{f_M} \nabla^2 f_M}^{\text{Diffusion}} + \overbrace{a_4}^{\text{Production}} - \overbrace{\lambda f_M}^{\text{Decay}} \tag{16}$$

2.6 Migration-inducing protein and inhibition

Mason et al. (2001) postulated that it is the combination of the migration-inducing effect of MIA in the RMS and the migration-inhibiting effect of SLIT in the SVZ that causes the motion of neuroblasts away from the SVZ towards the OB. Although a high concentration of SLIT at the edges of the SVZ prevents the migration of neuroblasts away from the RMS and the OB, the presence of MIA in the RMS encourages migration into the RMS. To simulate this, Equations (13)–(16) were combined into the following set of equations:

$$\frac{\partial n_A}{\partial t} = \overbrace{\nabla\left(\frac{\delta_A(1 + f_M)}{1 + f_I}\nabla n_A\right)}^{\text{Variable Diffusion}} + \beta_A(\mathbf{r}) n_A(1 - n_A) + \alpha_A n_C - \zeta(\mathbf{r}) n_A - (\gamma_A + \varepsilon(\mathbf{r})) n_A \tag{17}$$

$$\frac{\partial f_I}{\partial t} = \delta_{f_I} \nabla^2 f_I - \lambda f_I \tag{18}$$

$$\frac{\partial f_M}{\partial t} = \delta_{f_M} \nabla^2 f_M + a_4 - \lambda f_M. \tag{19}$$

2.7 Study overview

In summary, the hypotheses tested in all the described submodels (Sections 2.2–2.6) state that the migration of neuroblasts through the RMS could be accelerated by the

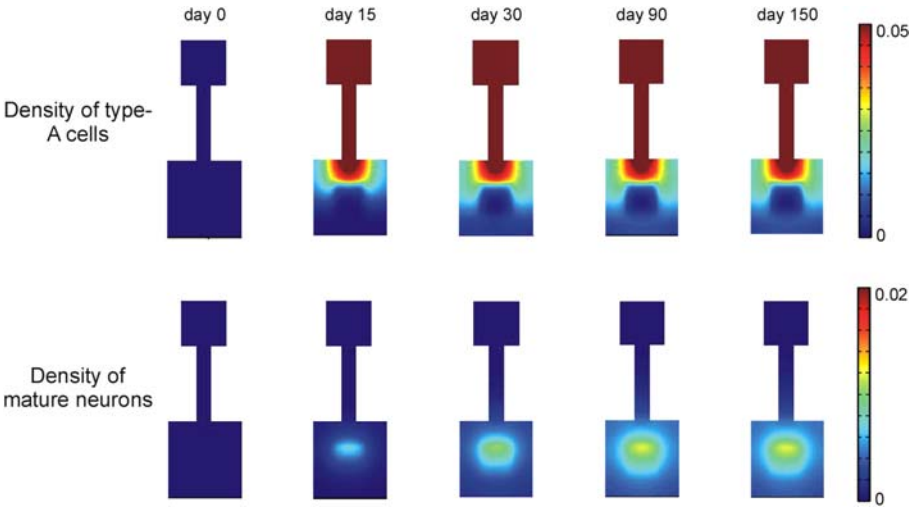

Figure 2. Representative snapshots ($t = 0$, 15, 30, 90 and 150 days) of type-A cell density (top) and cell density of mature neurons (bottom).

presence of one or more chemical factors. In this study, we tested the effect of a chemo-attractant (f_A), a chemo-repellent or inhibitor (SLIT), a migration-inducing factor (MIA) and a combination of several of these factors. Starting with a bioluminescent cell population in the SVZ, the simulations were run for a simulated period equivalent to 200 days. This corresponds to the time frame of the experimental follow-up (Reumers et al. 2008) and is sufficient for all the mechanisms to reach a steady state value.

Given the sloppy nature of the model, this study used the reference parameter values of Ashbourn et al. As such, the results obtained in this study must be interpreted in a qualitative way. To make the comparison between the various migratory models more valid, all parameters were chosen in such a way that the maximum concentration of f_A, MIA and SLIT was approximately equal to 10 (non-dimensional value). A sensitivity analysis was carried out in each case to assess the impact of the value of this maximal concentration (20% and 200% of reference) on the overall model behaviour.

3. Results

Figure 2 shows the results for the model simulating chemo-attraction. This model showed a relatively quick equilibration of n_B and n_C to their steady state values, and a steady migration of neuroblasts n_A towards the OB, where mature neurons n_N are formed in a central area until a maximum value was reached. After 200 days, all models have reached an equilibrium state, and Figure 3 shows the spatial distribution of the chemical factors (chemo-attractant, MIA and SLIT) in the different models at that point. It can be seen that the chemo-attractant factor is mainly present in the OB, whereas the highest concentration of SLIT can be found at the edges of the SVZ, and MIA is abundant in the RMS. For the cell concentrations, spatial and temporal behaviour similar to the chemo-attractant model was found in all our models, including the diffusion model. Neuroblast migration patterns through the RMS were similar in all models, although the magnitude and speed of the migration varied. Figure 4 shows the distribution of type-A cells and mature neurons at a fixed time $t = 200$ days.

As the simulations showed no variation in migration patterns in the different models, Figure 5 focuses on the average cell density in the OB. Cells present in the OB are either type-A neuroblasts n_A or fully mature neurons n_N. As the models only differ in the method of simulating migration, the average cell density in the OB gives a good indication of the speed of migration and the number of neurons formed during the process.

It should be noted that even when only diffusion is modelled, as is in our reference model, some migration will occur, although very slowly. It can also be seen that both chemo-attraction and chemorepulsion enhance

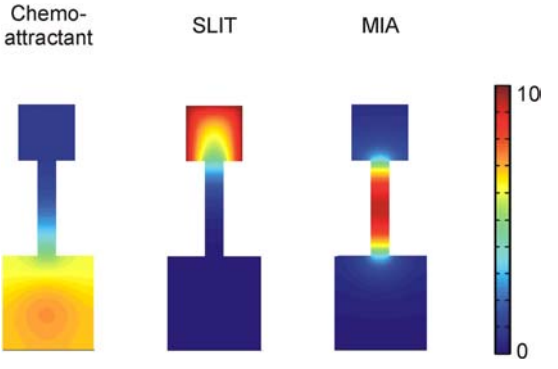

Figure 3. Equilibrium concentrations of f_A, SLIT and MIA in the relevant models; snapshots are taken at time $t = 200$ days.

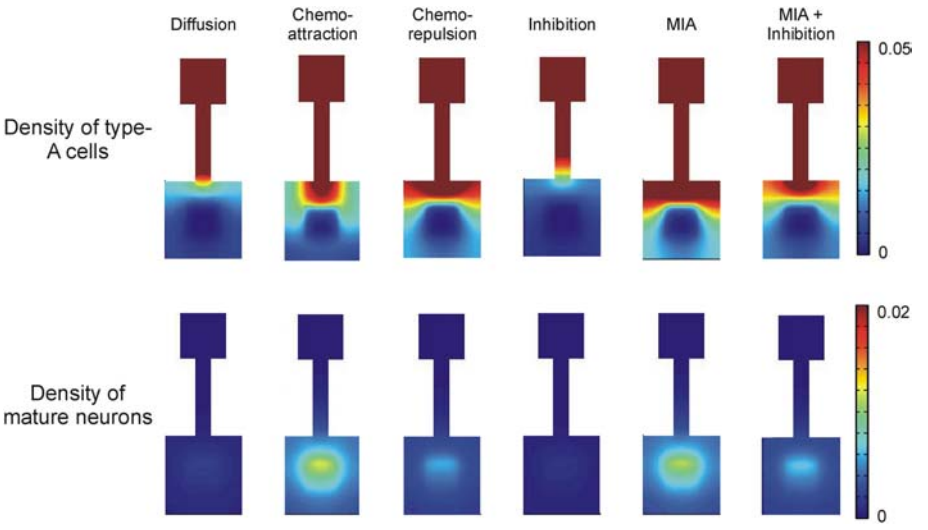

Figure 4. Comparison of the migration patterns in different models. Type-A cell density and density of mature neurons at time $t = 200$ days are shown.

migration considerably, but each in a different temporal pattern. The sensitivity analysis showed that even at different concentrations of f_A or SLIT, chemorepulsion always started slower. Furthermore, it was seen that in a chemorepulsive model, the average cell density in the OB reached at equilibrium was more strongly dependent on the maximum concentration of SLIT than on the chemo-attraction and MIA models (Figure 6), as in the later models, the final cell density increased less strongly with the increasing maximal concentration of the chemical.

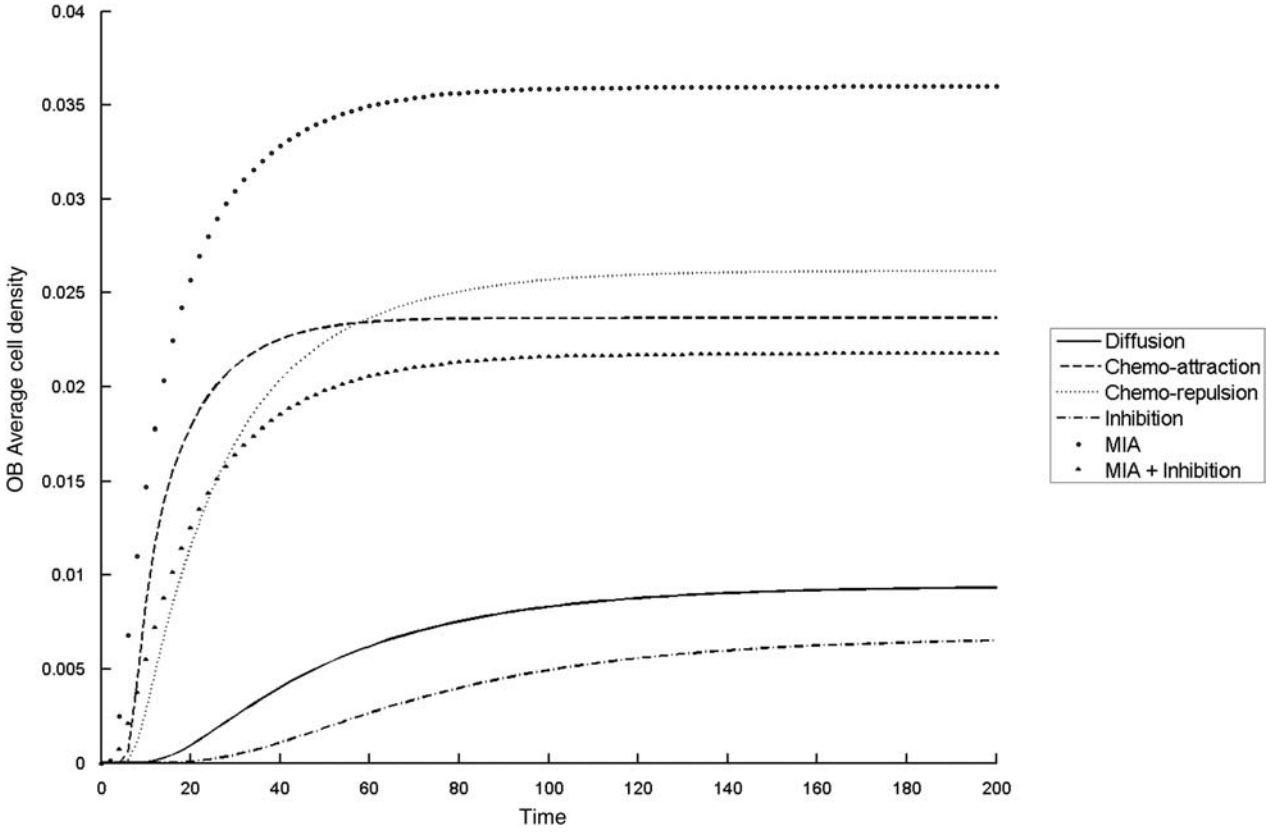

Figure 5. Temporal evolution of the average cell density within the OB for the different models. Cells in the OB are either type-A neuroblasts or mature neurons, and cell densities are shown in a non-dimensionalised form.

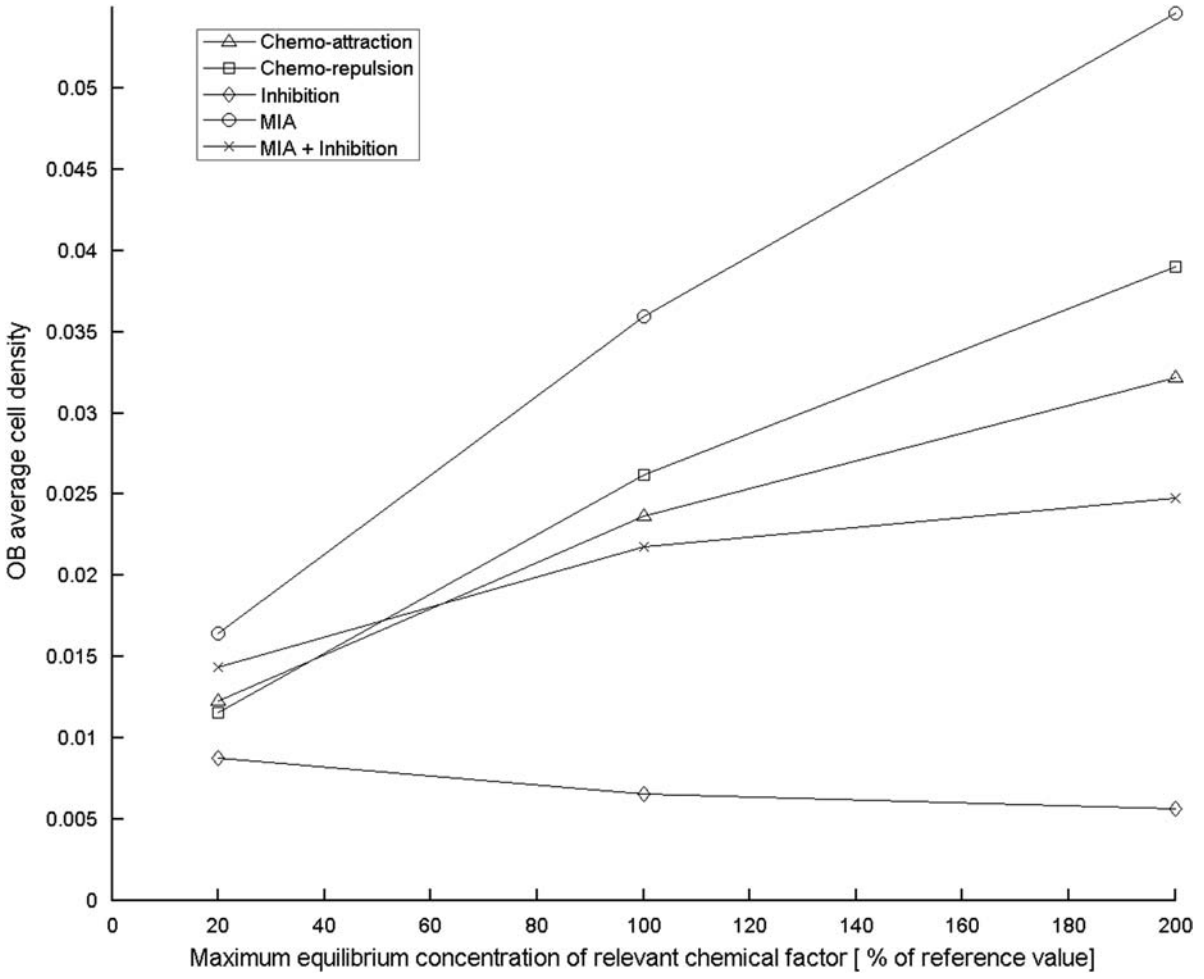

Figure 6. The effect of concentration of the relevant chemical factor (f_A, SLIT or MIA) in the different models on the average cell density in the OB at time $t = 200$ days. The concentration of the chemical factor was varied between 20% and 200% of the reference value.

The migration-inducing factor MIA was modelled to increase the diffusion constant δ_{n_A} of the type-A neuroblasts, affecting their mobility inside the RMS. As expected, this is also demonstrated in the results. In the presence of MIA, migration through diffusion is considerably accelerated. General inhibition was modelled to have the exact opposite effect on the diffusion constant. Figure 5 shows that the presence of SLIT, when modelled as the only chemical factor in the system, slows down migration, by limiting the mobility of the neuroblasts in the SVZ.

It was postulated that a high concentration of SLIT at the edges of the SVZ, combined with the presence of migrating-inducing factor MIA, would drive the type-A neuroblasts towards the OB. Results show that the average cell density predicted by the model in the presence of SLIT and MIA is increased in comparison with that of the reference model. In comparison with the model that includes only MIA, the density and speed of migration are, however, decreased.

To further investigate the effect of f_A, MIA and SLIT on migration, the average cell density in the OB at the end of the simulated period for various concentrations of the different chemical factors was calculated. The maximum equilibrium concentration of f_A, MIA and SLIT was varied in all the models between 20% and 200% of the reference value. It can be seen from Figure 6 that increasing the concentration of the relevant chemical factor (f_A, MIA and SLIT) in the chemoattraction model, the chemorepulsion model and the MIA-model enhances the migration of neuroblasts through the RMS. In the general inhibitor model, however, a higher concentration of SLIT further reduces the amount of migration.

4. Discussion

Neuronal migration in the postnatal brain is a highly directed motion, which suggests that it is regulated by very specific orienting cues. The exact nature of these cues is,

however, still under investigation. In this study, we investigate the different theories of migration of neuroblasts through the RMS, starting with the model developed by Ashbourn et al. (2012). One of the hypotheses constituting their model is that migration is mainly driven by chemotaxis. We postulated that other underlying causes could also explain the migration of neuroblasts through the RMS and into the OB.

We created a reference model in which only diffusion of the neuroblasts was present, but no directed motion was included, to serve as our reference model. Some comments must be made concerning this approach. First, diffusion is a random process in which cell types spread out over space. In this particular model, however, the diffusion is limited artificially by the presence of zero-flux boundary conditions at the edge of the model domain. So, although diffusion has no preferred direction, because of the definitions of the geometrical domain, a small concentration of type-A neuroblasts will migrate through the RMS and arrive at the OB, the exact amount depending on several parameters, e.g. the diffusion constant δ_{n_A} and the apoptosis constant γ_A. Therefore, a factor is assumed to enhance migration when, compared with the reference model, more neuroblasts migrate through the RMS. Second, in reality, the diffusion constant of type-A neuroblasts is not constant, but the motion of neuroblasts is influenced by the presence of other cells and by the structure of the extracellular matrix.

The models proposed in this study contain many parameters for which no values are available in the literature. Directly measuring them is often difficult and sometimes even impossible. Fitting the model outcome to experimental results would be a possibility, but usually results in large parameter uncertainties. Furthermore, several parameter combinations can result in the same outcome. However, it has been shown extensively in the literature that collective fitting in biological models could yield well-constrained predictions even when it left individual parameters very poorly constrained (Gutenkunst et al. 2007a, 2007b; Daniels et al. 2008). This is particularly true in sloppy models. In such models, many parameter combinations can lead to the same outcome, whereas there is no clear distinction between important and unimportant parameters (Gutenkunst et al. 2007a). By changing a combination of parameters, the outcome remains unchanged, but there is no single parameter that has a negligible effect on the results. The model can thus not be simplified, and parameter fitting becomes a complex task. Ashbourn et al. (2012) confirmed the sloppy nature of the neurogenesis model, indicating that we should focus on predictions rather than on individual parameters. These results justify the assumptions made with regard to the unknown parameters in the different migration models of this study. To avoid introducing new parameters into the model, we used the same parameters that were used for the chemo-attractant factor in the model of Ashbourn et al. (2012) for SLIT and MIA with some small adjustments wherever necessary.

Several hypotheses exist concerning the nature of the cues guiding type-A neuroblasts through the RMS. One suggestion is the presence of a chemo-attractant factor in the OB (Bloch-Gallego et al. 1999; Yee et al. 1999; Alcantara et al. 2000; Ghashghaei et al. 2007), sometimes identified to be netrin-1 (Murase and Horwitz (2002)). This is the assumption made by Ashbourn et al. (2012) in their chemo-attractant model. However, experiments showed that the migration of neuroblasts continues to occur towards the RMS, even after there has been a surgical removal of the OB (Jankovski et al. 1998), thus indicating that long-distance attractive signals from the OB are not necessary for oriented migration. A different hypothesis encountered in the literature states that chemorepulsive cues might play a role in the process. SLIT proteins, produced by cells surrounding the SVZ, have been shown to repulse newly generated cells from the SVZ (Hu 1999; Wu et al. 1999; Ghashghaei et al. 2007). This process was modelled in our chemorepulsive model by imposing Dirichlet boundary conditions for the SLIT concentration at the edges of the SVZ. Our model showed that chemorepulsion could indeed be a cause of neuronal migration, by pushing the newly formed type-A neuroblasts away from the SVZ and into the RMS. It was also shown that the effect of chemo-attraction and chemorepulsion was comparable, and both migration mechanisms were found to be plausible hypotheses.

Recently, glial cells in the RMS have been implicated as the source of a protein with migration-inducing activity (Mason et al. 2001). The exact nature of this protein, referred to as MIA, is yet to be determined, but the protein was shown to initiate cell migration and facilitate cell movement through the RMS. This was modelled by making the diffusion constant of type-A neuroblasts proportional to the concentration of MIA. Our model showed that the presence of MIA in the RMS would greatly increase the amount of cells migrating through the RMS. It is important to note, however, that this result is completely dependent on the modelling of random diffusion. As mentioned before, even with only the diffusion model, the mathematical model will allow some migration towards the OB, in part due to the definition of the geometrical domain. The presence of MIA increases this diffusion, but does not allow for a diffusion-independent motion of cells. This is in contrast to the chemo-attraction and chemo-repulsion models discussed above, which do allow diffusion-independent migration by the cells.

Mason et al. (2001) observed that SLIT does not necessarily act as a repulsive cue, but rather as an inhibitor. They showed that in the presence of high concentrations of SLIT, cells ceased all movement, and their results suggested that it is the combination of SLIT and MIA that acts as a chemorepulsive cue. To investigate this

claim, we created a general inhibitor model with SLIT being the only factor present and a model combining the effects of MIA and SLIT.

Our results confirm that the inhibitory effect of SLIT on its own cannot explain the directed migration through the RMS. Although the inhibitory effect of SLIT, combined with the spatial orientation of the SLIT gradient, does favour motion towards the RMS, the total amount of migration is always reduced by the presence of SLIT itself when compared with the reference model. Similar results were obtained from the combined MIA/SLIT model. The combination of MIA and SLIT does lead to a chemorepulsive response, leading neuroblasts away from the SVZ towards the OB, but the migration was reduced in comparison with the model that only simulated the presence of MIA. It should, however, be noted that part of this result can again be explained by the artificial boundary conditions. In reality, part of the importance of SLIT in the guidance of migration is to keep the cells inside the SVZ by inhibiting their motion in other directions and thus indirectly pushing the cells towards the entrance of the RMS. In the model, this purpose is achieved by the boundary conditions. As explained previously, without boundary conditions, directed migration towards the OB cannot be explained by diffusion alone. It is thus very possible that the presence of SLIT as an inhibitor is essential to the directed migration of neuroblasts in vivo, acting as some sort of chemical boundary, guiding random diffusion towards the OB.

5. Conclusion

In this study, we have developed a mathematical model to investigate the directed neuronal migration in the postnatal brain and its regulation by specific orienting cues. We believe that, together with experimental results, this model can lead to a better understanding of subventricular neurogenesis. Using the model, hypotheses can be refined and corrected, and input for the design of further experiments can be formulated. Starting from the reference model of Ashbourn et al. (2012), we implemented different theories of migration of neuroblasts through the RMS, including chemo-attraction, chemorepulsion, general inhibition and the presence of a migration-inducing protein. Apart from the general inhibition model, all the models were able to provide good results, in qualitative correspondence with the experimental observations.

Acknowledgements

AVS is a Fellow of the Research Foundation Flanders (FWO). The authors acknowledge support from the Nuffield Foundation through the awards of Undergraduate Research Bursaries URB/39423 and URB/37878 (for R.B. and J.J.M., respectively) and from the European Research Council under the European Union's Seventh Framework Programme (FP7/2007-2013)/ERC grant agreement No. 279100 (A.V.S. and L.G.).

References

Alcantara S, Ruiz M, De CF, Soriano E, Sotelo C. 2000. Netrin 1 acts as an attractive or as a repulsive cue for distinct migrating neurons during the development of the cerebellar system. Development. 127(7):1359–1372.

Ashbourn JM, Miller JJ, Reumers V, Baekelandt V, Geris L. 2012. A mathematical model of adult subventricular neurogenesis. J R Soc Interface. 9(75):2414–2423.

Biebl M, Cooper CM, Winkler J, Kuhn HG. 2000. Analysis of neurogenesis and programmed cell death reveals a self-renewing capacity in the adult rat brain. Neurosci Lett. 291(1):17–20.

Bloch-Gallego E, Ezan F, Tessier-Lavigne M, Sotelo C. 1999. Floor plate and netrin-1 are involved in the migration and survival of inferior olivary neurons. J Neurosci. 19(11):4407–4420.

Daniels BC, Chen YJ, Sethna JP, Gutenkunst RN, Myers CR. 2008. Sloppiness, robustness, and evolvability in systems biology. Curr Opin Biotechnol. 19(4):389–395.

Geris L, Gerisch A, Sloten JV, Weiner R, Oosterwyck HV. 2008. Angiogenesis in bone fracture healing: a bioregulatory model. J Theor Biol. 251(1):137–158.

Gerisch A, Chaplain MA. 2006. Robust numerical methods for taxis-diffusion-reaction systems: applications to biomedical problems. Math Comput Model. 43:49–75.

Ghashghaei HT, Lai C, Anton ES. 2007. Neuronal migration in the adult brain: are we there yet? Nat Rev Neurosci. 8(2):141–151 (doi:10.1038/nrn2074).

Gutenkunst RN, Casey FP, Waterfall JJ, Myers CR, Sethna JP. 2007b. Reverse engineering biological networks, opportunities and challenges in computational methods for pathway interference. Ann NY Acad Sci. 1115:203–211.

Gutenkunst RN, Waterfall JJ, Casey FP, Brown KS, Myers CR, Sethna JP. 2007a. Universally sloppy parameter sensitivities in systems biology models. PLoS Comput Biol. 3(10):1871–1878.

Hu H. 1999. Chemorepulsion of neuronal migration by Slit2 in the developing mammalian forebrain. Neuron. 23(4):703–711.

Jankovski A, Garcia C, Soriano E, Sotelo C. 1998. Proliferation, migration and differentiation of neuronal progenitor cells in the adult mouse subventricular zone surgically separated from its olfactory bulb. Eur J Neurosci. 10(12):3853–3868.

Lledo P, Alonso M, Grubb M. 2006. Adult neurogenesis and functional plasticity in neuronal circuits. Nat Rev Neurosci. 7(3):179–193.

Lois C, Alvarez-Buylla A. 1993. Proliferating subventricular zone cells in the adult mammalian forebrain can differentiate into neurons and glia. Proc Natl Acad Sci USA. 90:2074–2077.

Lois C, Garcia-Verdugo JM, Alvarez-Buylla A. 1996. Chain migration of neuronal precursors. Science. 271(5251):978.

Luskin MB. 1993. Restricted proliferation and migration of postnatally generated neurons derived from the forebrain subventricular zone. Neuron. 11:173–189.

Marillat V, Cases O, Nguyen-Ba-Charvet KT, Tessier-Lavigne M, Sotelo C, Chedotal A. 2002. Spatiotemporal expression patterns of slit and robo genes in the rat brain. J Comp Neurol. 442(2):130–155.

Mason HA, Ito S, Corfas G. 2001. Extracellular signals that regulate the tangential migration of olfactory bulb neuronal precursors: inducers, inhibitors, and repellents. J Neurosci. 21(19):7654–7663.

Murase S, Horwitz AF. 2002. Deleted in colorectal carcinoma and differentially expressed integrins mediate the directional migration of neural precursors in the rostral migratory stream. J Neurosci. 22(9):3568–3579.

Nguyen-Ba-Charvet KT, Picard-Riera N, Tessier-Lavigne M, Baron-Van EA, Sotelo C, Chedotal A. 2004. Multiple roles for slits in the control of cell migration in the rostral migratory stream. J Neurosci. 24(6):1497–1506.

Reumers V, Deroose CM, Krylyshkina O, Nuyts J, Geraerts M, Mortelmans L, Gijsbers R, Van den Haute C, Debyser Z, Baekelandt V. 2008. Noninvasive and quantitative monitoring of adult neuronal stem cell migration in mouse brain using bioluminescence imaging. Stem Cells. 26(9):2382–2390.

Smith MCM. 1998. Cell cycle length of olfactory bulb neuronal progenitors in the rostral migratory stream. Dev Dyn. 213:220–227.

Taupin P, Gage FH. 2002. Adult neurogenesis and neural stem cells of the central nervous system in mammals. J Neurosci Res. 69:745–749.

Weiner R, Schmitt BA, Podhaisky H. 1997. ROWMAP - a ROW-code with Krylov techniques for large stiff ODEs. Appl Numer Math. 25:303–319.

Wu W, Wong K, Chen J, Jiang Z, Dupuis S, Wu JY, Rao Y. 1999. Directional guidance of neuronal migration in the olfactory system by the protein Slit. Nature. 400(6742):331–336.

Yee KT, Simon HH, Tessier-Lavigne M, O'Leary DM. 1999. Extension of long leading processes and neuronal migration in the mammalian brain directed by the chemoattractant netrin-1. Neuron. 24(3):607–622.